Evaluation of nitrogen- and silicon-vacancy defect centres as single photon sources in quantum key distribution

2014 New J. Phys. 16 023021

(http://iopscience.iop.org/1367-2630/16/2/023021)

New Journal of Physics
The open access journal at the forefront of physics
Deutsche Physikalische Gesellschaft DPG | IOP Institute of Physics

Evaluation of nitrogen- and silicon-vacancy defect centres as single photon sources in quantum key distribution

Matthias Leifgen[1,5], Tim Schröder[1,6], Friedemann Gädeke[1], Robert Riemann[1], Valentin Métillon[2], Elke Neu[3,7], Christian Hepp[3], Carsten Arend[3], Christoph Becher[3], Kristian Lauritsen[4] and Oliver Benson[1]

[1] Nano-Optik, Institut für Physik, Humboldt-Universität zu Berlin, 12489 Berlin, Germany
[2] École normale supérieure, 45 rue d'Ulm, Paris, France
[3] Fachrichtung 7.2 (Experimentalphysik), Universität des Saarlandes, Campus E2.6, 66123 Saarbücken, Germany
[4] PicoQuant GmbH, Rudower Chaussee 29, 12489 Berlin, Germany
E-mail: leifgen@physik.hu-berlin.de and schroder@mit.edu

Received 6 September 2013, revised 9 January 2014
Accepted for publication 10 January 2014
Published 13 February 2014
New Journal of Physics **16** (2014) 023021
doi:10.1088/1367-2630/16/2/023021

Abstract

We demonstrate a quantum key distribution (QKD) testbed for room temperature single photon sources based on defect centres in diamond. A BB84 protocol over a short free-space transmission line is implemented. The performance of nitrogen-vacancy (NV) as well as silicon-vacancy defect (SiV) centres is evaluated. An extrapolation for the future applicability of such sources in quantum information processing is discussed.

[5] Author to whom any correspondence should be addressed.
[6] Present address: Department of Electrical Engineering and Computer Science, Massachusetts Institute of Technology, Cambridge, Massachusetts 02139, USA.
[7] Present address: Universität Basel, Departement Physik, Klingelberstrasse 82, 4056 Basel, Switzerland.

1. Introduction

Single photons are a key ingredient in many quantum information processing (QIP) applications. Examples are quantum key distribution (QKD) [1], long distance quantum repeater protocols [2] or linear optical quantum computing. However, in QKD, high key rate and/or long distance experiments have been successfully implemented without true single photons using weak coherent laser pulses (WCP) [3, 4] together with the decoy state protocol [5, 6]. Although this protocol is secure against photon number splitting (PNS) attacks, it has the disadvantage of producing some overhead, because one explicitly uses vacuum and very low intensity pulses together with the signal pulses and also operates with faint pulses with a mean photon number per pulse of around 0.5. In addition, long-range QKD requires quantum repeaters where sources of single indistinguishable photons are advantageous over photon pair sources [2]. A true single photon source (SPS) with high efficiency could therefore still be favourable in QIP compared to WCP. Efficiency means that it emits a single photon into a well-defined spectral and spatial mode with a probability near unity each time a trigger is applied. A practical SPS should also have a stable emission rate, be easy-to-use, should operate at room temperature and at high repetition frequencies.

The most promising candidates for practical true SPS today are solid-state emitters, such as quantum dots (QDs) [7, 8] or defect centres in diamond [9, 10]. QDs are available for a broad range of wavelengths, including the telecom bands, can be excited optically or electrically and are efficient, with coupling rates to a usable output mode of up to over 70% [11]. One major drawback of QDs is until now the need for cryogenic cooling. Regarding defect centres in diamond, the most intensely studied defect centre is the nitrogen-vacancy (NV) centre [9]. It is formed by a substitutional nitrogen atom together with an adjacent vacancy. The NV centre occurs in a neutral and a charged state [12]. In the following we only regard the negatively charged NV centre. Its electronic structure is well understood [13, 14] and can be described by a three-level model concerning its optical properties. Optical and electrical (neutral NV) excitation was demonstrated [15, 16]. Also, another defect centre, the silicon-vacancy (SiV) centre has been studied [10, 17]. It consists of a silicon impurity in a so-called split-vacancy-configuration [18]. One key feature of defect centres is their optical stability and high quantum yield even at room temperature. Whereas emission into the zero phonon line (ZPL) is a few per cent for the NV centre (3% at cryogenic temperatures [19]), the SiV emits 70–80% of photons into the ZPL. Both for NV and SiV centres high photon generation rates have been reported, for the NV exceeding 2 Mcps [20], for the SiV exceeding 6 Mcps [10], all under continuous laser excitation. Other, presumably Cr-related centres with potentially even higher count rates have been investigated [21, 22], but their reliable fabrication is problematic and a full understanding of their structural properties is missing. So far only the NV centre has been utilized as SPS in a QKD experiment [23, 24].

In order to evaluate the applicability of defect centres as reliable sources for QIP, in particular for QKD, it is desirable to use test-beds that allow for long-term measurements, implementation of different protocols, as well as straightforward integration of different defect centres. In this paper, we report the realization of such a testbed. It consists of a short free-space transmission line combined with a compact SPS based on defect centres. The source relies on a specialized confocal setup for stable optical excitation and efficient collection of single photons from defect centres. Furthermore, it is designed in a way that it is easy to replace one kind of defect centre by another. QKD experiments are performed with NV centres and for the first time also with SiV centres.

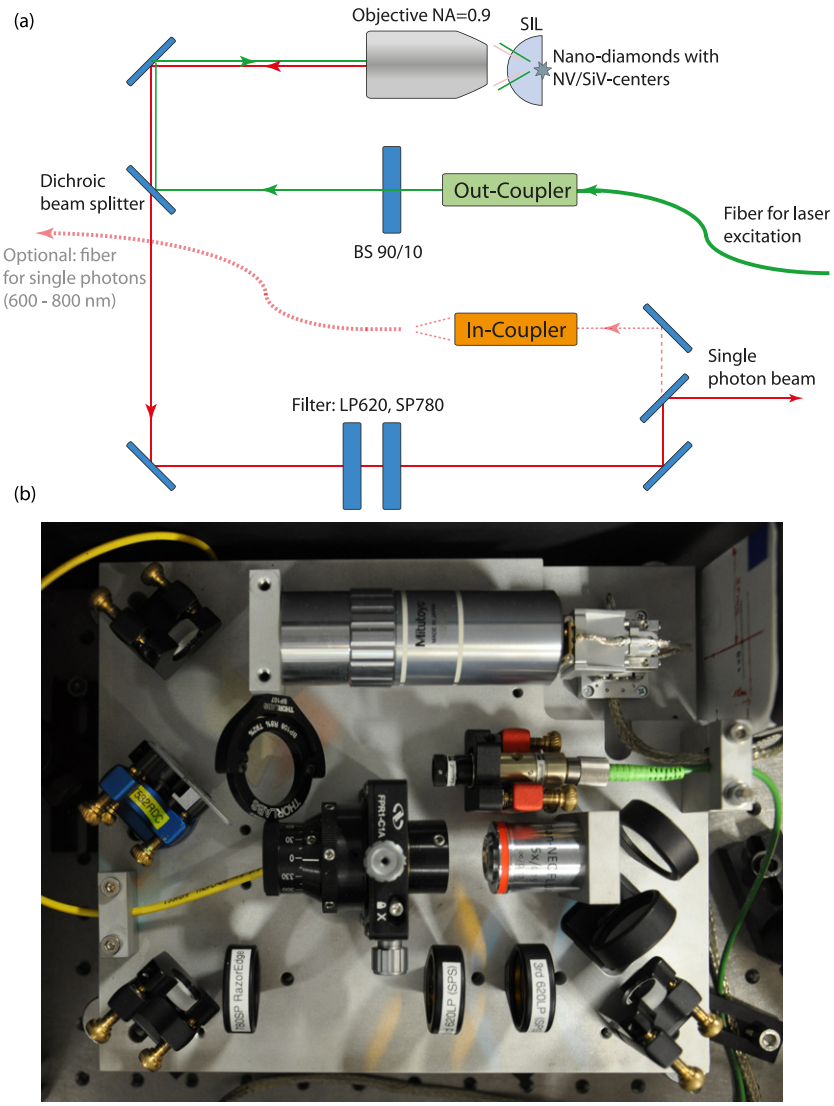

Figure 1. (a) Scheme and (b) photo of the compact confocal setup. The excitation laser is focused with a high NA objective onto the sample which is either one of several nanodiamonds spin-coated on a SIL or grown on a substrate. The emission is collected by the same objective and then filtered by a dichroic beam splitter (exchangeable) and longpass (LP) and shortpass (SP) filters to clean it from residual laser light or fluorescence of the SIL or the substrate.

2. Compact and versatile design of the single photon source

The design of the source relies on a compact, portable and ready to use confocal setup. A ZrO_2 solid immersion lens (SIL) can be utilized to enhance the collection of single photons emitted from defect centres in nanodiamonds (NDs) spin-coated directly on the SIL. Details of the fabrication of SILs with NV centres are provided in [20]. The source is built for single photon emitters with a wavelength range from 600 to 800 nm. With this it allows for the implementation of SPS using NV, SiV as well as Cr-based defect centres. Figure 1 shows a schematic (a) and a

photograph (b) of the source which fits completely on an aluminum plate and has dimensions of only 22.5 cm × 19 cm × 9 cm. In this way, the SPS is mobile and can easily be integrated in different experimental setups. The setup is robust against mechanical vibrations and thermal drifts due to its small size and compact mounting of all optical components. The generated single photon beam can either be free space or fibre coupled by removal/addition of a single mirror which is equipped with a magnetic base. The sample unit holding the defect centres can either be the SIL with spin-coated defect centres or a substrate containing defect centres due to a removable sample holder. The setup is equipped with broadband optics and thus suitable for various defect centres, provided their emission wavelength is in the range of 600–800 nm. Only the exchangeable dichroic mirror has to be adapted together with the suitable excitation source and matched filters. The sample holder is mounted on a 3-axes piezo stage. In order to keep track of the absolute position of the stage, sensors capable of detecting changes on a nanometre scale are used (SmarAct System). With this system it is possible to focus on a well-defined position on the sample with very high accuracy and stability.

3. Properties of colour centres used in the single photon source

In principle, any kind of colour centre can be employed in the source described in the previous section. In the following, we focus on NV and silicon-vacancy (SiV) centres.

3.1. Nitrogen-vacancy centres in diamonds as single photon source

NVs have been proven to be stable and bright single photon emitters and have been extensively studied and described elsewhere [9, 20, 25]. They have a broad emission spectrum from 600 to 800 nm. High count rates of up to 2.4 Mcps (cw excitation) and relatively high overall photon yields (the ratio between excitation and detection rates) of up to 4.2% have been achieved [20]. The quality of single photon emission, in particular the contribution of multi-photon events is routinely determined by measuring the second-order autocorrelation function ($g^{(2)}(\tau)$) in a Hanbury–Brown Twiss (HBT) setup [26]. Although in the ideal case $g^{(2)}(\tau = 0) = 0$, a value of $g^{(2)}(\tau = 0) < 0.5$ is generally accepted as a criterion for single photon emission. Values below 0.12 have been reported with NV defect centres [20]. In QKD it is favourable to have photons at a well-defined instant of time, thus pulsed excitation of the defect centres is of interest. In such a pulsed excitation scheme, using a green diode laser (PicoQuant LDH-P-FA-530 [27], 531 nm, pulse width <100 ps), we achieved count rates of 8900 cps at an excitation rate of 1 MHz for an NV centre in a ND which was spin-coated on a SIL. This corresponds to an overall photon yield of 0.89% and a source efficiency of 2.9%. The latter is defined as the ratio of excitation pulses resulting in a single photon without background in the desired optical mode, here the free space beam of the QKD experiment. This value is determined for a given overall photon yield by taking the overall transmission η_{setup} of 0.31 of our setup, including the efficiency of ∼65% of the avalanche photodiodes (APDs), into account. For the QKD experiment, the maximal excitation rate was limited to frequencies up to 1 MHz by the modulation rate of the electro-optical modulator (EOM) (see section 4). A $g^{(2)}(0)$ value under pulsed excitation of 0.09, clearly indicating high purity single photon emission, is measured (figure 2(a)) using high resolution time-correlation electronics (PicoHarp 300 from PicoQuant). A lifetime of 28.5 ± 1.5 ns is calculated from the pulse shape.

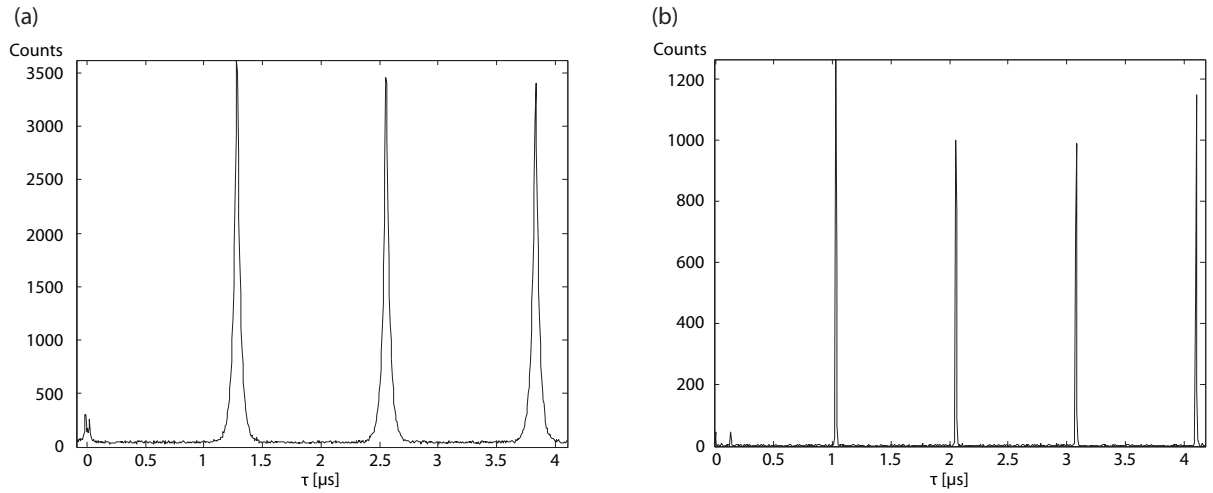

Figure 2. Measured intensities as a function of time for NV (a) and SiV (b) emission under pulsed excitation to calculate $g^{(2)}(\tau)$. The excitation rates were 800 kHz and 1 MHz, respectively. The missing pulse at $\tau = 0$ indicates single photon emission. From the pulse shape we calculated a lifetime of the excited state of 28.5 ± 1.5 ns for the NV and 3 ± 2 ns for the SiV.

3.2. Silicon-vacancy centres in diamonds as single photon source

A disadvantage of the NVs is their phonon-broadened emission spectrum and long lifetime in the order of 20 ns, which limits the maximal excitation and emission rate. SiVs have a much narrower, linearly polarized emission spectrum of about 1–2 nm at around 739 nm [10], due to lower phonon coupling and a concentration of the emission into the ZPL, and a shorter lifetime in the order of 1 ns, making them an interesting candidate for QKD with single photons, especially for free space daylight operations [28]. There have been reports on high photon emission rates of up to 6.2 Mcps using cw excitation and values of $g^{(2)}(0)$ below 0.05 [17]. Single SiV centres are created during chemical vapour deposition (CVD) growth of randomly oriented NDs on iridium (Ir) films [10]. We excite our SiV sample with laser pulses from a red diode laser (PicoQuant diode laser LDH-D-C-690, 687 nm, pulse width <100 ps) at an excitation frequency of 1 MHz. With the brightest SiV centre we achieved a photon count rate of 3700 cps and a $g^{(2)}(0)$ value of 0.04, see figure 2(b). From the pulse shape, a lifetime of 3 ± 2 ns is calculated. The overall photon yield was 0.37% and the plain source efficiency is thus 1.2%. The achievable count rate per excitation pulse was lower for the SiV centre compared to the NV centre. Knowing that the collection efficiency of emitted photons from SiV NDs grown on Ir-substrate can be very high [17], this hints a lower quantum efficiency. In [17], a quantum efficiency between 1 and 9% was estimated. Compared to the NV centre, the excitation frequency could be chosen to be much higher for the SiV centre due to the shorter lifetime, which could compensate for the lower quantum efficiency (cf section 6).

It is also observed that SiVs do not have the same stability as NVs under excitation. Some of them bleach, probably due to photo-ionization, especially when excited at higher excitation powers. It has been suggested to circumvent bleaching by creating free electrons close to the sample by shining a blue laser at its vicinity [29]. Using surface treatment or a better control of the impurity content of the samples might also be a way to produce more photostable SiVs in the future [17].

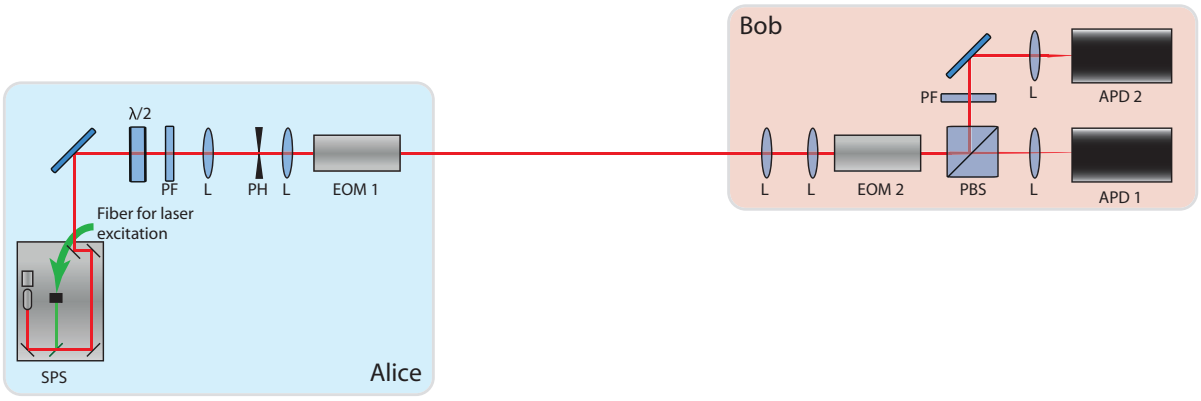

Figure 3. Schematics of the QKD testbed. On Alice's side, single photons are emitted from the source (SPS) and prepared in a well-defined polarization state by a $\lambda/2$ plate and a polarization filter (PF). After collimation and spatial mode cleaning by two lenses (L) and a pinhole (PH), they pass through an electro-optical modulator (EOM 1). On Bob's side, the beam is recollimated by two lenses and then passes through a second modulator (EOM 2). Then, the polarization is analysed by a PBS and a polarization filter in the reflected mode of the PBS, which has a slightly reduced contrast compared to the transmitted mode. After passing through a lens for focusing, the photons are detected on one of two APDs.

4. Setup of QKD testbed

The setup is shown in figure 3. The emitted free space photons from the SPS are initially prepared in a linear polarization state by passing through a linear polarization filter after a $\lambda/2$ plate which is adjusted to maximize the count rate. After passing through a pinhole for further spatial mode cleaning, the photons impinge on the first EOM which is controlled by Alice. The EOM acts as a $\lambda/2$ and $\lambda/4$ plate, respectively, depending on the applied voltage. In this way two orthogonal linearly polarized photon states as well as two orthogonal circular polarization states can be encoded on the incoming photons, compliant to the BB84 protocol [30]. After passing through a lens system for recollimation, the photons pass through a second EOM, which is controlled by Bob. Bob randomly chooses a measurement basis by setting the voltage such that the EOM either does not modify the photons or acts as a $\lambda/4$ plate. A circular polarization is thus transformed into a linear one or vice versa. The linear polarization state can then be deterministically analysed in a system consisting of a polarizing beam splitter (PBS), a linear polarization filter, compensating the non-perfect contrast of the PBS in reflection, and two APDs (Perkin Elmer AQR). For the random bit and basis choice of Alice and Bob, quantum random numbers from the online random number service of HU Berlin and PicoQuant GmbH[8] are used. The EOM is constructed in a way that it acts as a zero order waveplate. This minimizes its wavelength dependency during the modulation of different polarization states. However, especially when using the broadband NV centre as light source, possible dependencies between wavelength and transmitted polarization state could open the door to side-channel attacks which would have to be analysed in a way similar to the analysis of multiphotons (cf section 5 below, especially the notion of 'tagged' photons). However, a thorough analysis of this problem is beyond the scope of this paper.

[8] QRNG online: http://qrng.physik.hu-berlin.de, see also [31].

Table 1. Results of the QKD experiments with NVs and SiVs, each run for 300 s.

	NV	SiV
Repetition rate	1 MHz	1 MHz
Count rate	8.9 ± 0.1 kbit s^{-1}	3.70 ± 0.04 kbit s^{-1}
Sifted key rate	3.99 ± 0.05 kbit s^{-1}	1.51 ± 0.02 kbit s^{-1}
QBER	$3.0 \pm 0.2\%$	$3.2 \pm 0.2\%$
Secured key rate	2.6 kbit s^{-1}	1 kbit s^{-1}

5. Experimental results

In order to test the suitability of two different single photon sources we ran the BB84 protocol in the QKD setup.

The experimentally obtained parameters are summarized in table 1. With the brightest NV centre, emitting at a count rate of 8.9 kcps, a sifted key rate of 3.99 kbit s^{-1} at a quantum bit error ratio (QBER) of 3% was achieved. The raw key was then further processed using the CASCADE protocol [32], resulting in a secure key rate of 2.6 kbit s^{-1}. The CASCADE protocol is an efficient post-processing protocol for the sifted key aiming at minimizing discrepancies between Alice and Bobs keys while at the same time minimizing Eves possible information about it. It consists of two steps: error correction by parity comparison between Alice and Bob and subsequent dilution of Eves information in the so-called privacy amplification. This privacy amplification is realized by a randomly chosen function belonging to a special class of hash functions. The algorithm which was used here was implemented by ourselves and can be downloaded on our website[9]. The observed QBER can be explained by the limited contrast of the polarization optics and the EOMs. The sifted keyrate would be comparable to the ones reported in previous QKD experiments with NV centres [23, 24] if one would account for the lower repetition frequency used here due to technical reasons by using a scaling factor. The secured keyrate however would fall short of the one reported for the aforementioned experiments because of a slightly higher QBER in our experiment and thus a more keybit consuming postprocessing.

Using the brightest stable SiV, emitting at a count rate of 3.7 kcps, we found a sifted key rate of 1.51 kbit s^{-1}, a QBER of 3.2% and a resulting secure key rate of 1 kbit s^{-1}. Both keys were transmitted at an experimental clock rate of 1 MHz.

Both NV and SiV centres were running with a stable emission rate over several hours, which was the necessary time to find the right EOM settings for transmission. This shows the long-term stability of our setup.

It is interesting to have a look at the source efficiencies and the $g^{(2)}(0)$ values of the SPS and their consequences on security concerning multiphoton events. An upper bound on the probability p_{m} to have multiphoton events in pulses emitted from a sub-Poisson light source is given by [33],

$$p_{\mathrm{m}} \leqslant \frac{\mu^2 g^{(2)}(0)}{2}, \tag{1}$$

where μ is the mean photon number per pulse which is identical to the efficiency of the SPS to emit a single photon into the desired mode. This upper bound can then be used to calculate a

[9] CASCADE online: http://www.physik.hu-berlin.de/nano.

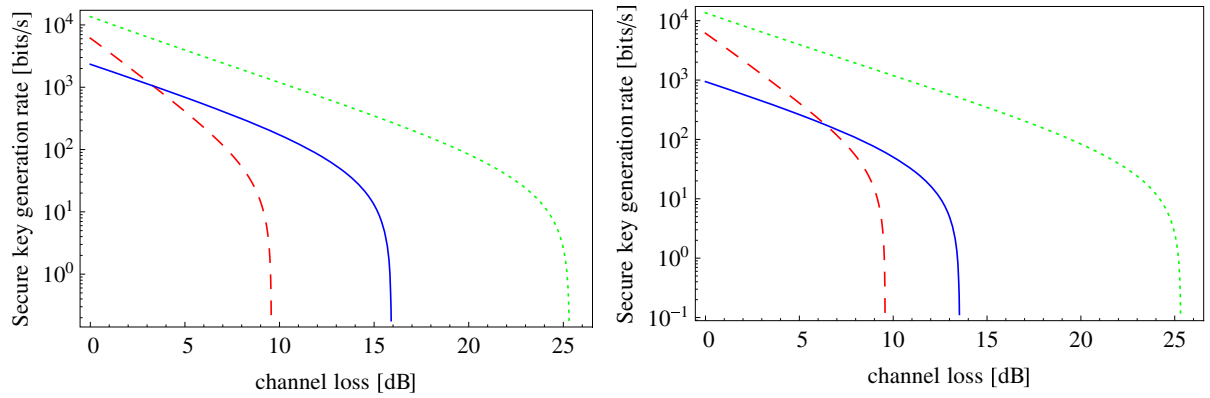

Figure 4. Secure key rates as a function of channel loss achieved with the BB84 protocol utilizing a true SPS with an NV centre (a) and a SiV centre (b) in blue. For comparison, the key rate when using an attenuated laser without the decoy state protocol at the optimized mean photon number $\mu \sim \eta_{\text{total}}$, where η_{total} is the overall transmission of the setup, is shown in red and dashed. Also shown in green and dotted is the secure key rate when using WCP together with the decoy state protocol with a mean photon number of 0.5 (calculated as in [37]).

lower bound on the secure key rate R, which takes the insecurity of having multiphoton events into account [34]:

$$R \geqslant q\{-Q_\mu f(E_\mu) H_2(E_\mu) + Q_\mu(1-\Delta)(1-H_2(E_\mu/(1-\Delta))\}. \tag{2}$$

In this formula, q is an efficiency factor depending on the exact protocol and expresses the randomness of the base choice, here it is $1/2$, Q_μ, the signal gain, is the fraction of detection events at Bob's side which is related to the signal with mean photon number μ[10], f is the error correction efficiency of the post-processing protocol and assumes a typical value of 1.22, E_μ is the error rate of a signal with mean photon number μ, and $H_2(x)$[11] is the binary Shannon information function [35]. Δ is the ratio of 'tagged' photons. 'Tagged' photons are photon qubits emitted by a faulty source, wearing a 'tag' with readable information for the eavesdropper revealing the actual basis of the qubit, cf [34]. When more than one photon is emitted at a time, it carries the same information as its partner photon and can be regarded as a 'tagged' photon when exploited by Eve in a PNS attack. For a single photon source, $\Delta = p_{\text{m}}/p_{\text{click}}$, with the detection probability of a signal $p_{\text{click}} \approx \mu \cdot \eta_{\text{total}} + p_{\text{dc}}$ [33]. η_{total} contains, besides the setup transmission η_{setup} (cf section 3.1), the transmission of the quantum channel. The dark count probability p_{dc} is in our setup 2.4×10^{-5}. Figure 4 shows the results of these secure key rate calculations as a function of the channel loss.

The secure key generation rate at 0 dB roughly reproduces our measured key rate after post-processing. For comparison we also plotted the secure key rate of a potential experiment with identical parameters (please note that for lasers repetition rates might be chosen to be higher than particularly for the NV SPS), but with an attenuated laser instead of a single photon source with a mean photon number of $\mu \sim \eta_{\text{total}}$, which is approximately optimal for an attenuated laser without the decoy state protocol and when considering possible PNS attacks [36]. The key rate is calculated as in equation (2), taking the multiphoton probability of a Poissonian light source into account. Also, the key rate of an identical experiment with an attenuated laser

[10] For an exact definition of Q_μ, see [6].
[11] $H_2(x) = -x\log_2(x) - (1-x)\log_2(1-x)$.

source together with the decoy state protocol (the used mean photon number of 0.5 is calculated as in [37]) is shown. At low loss, attenuated laser pulses without the decoy state protocol have relatively high signal intensities and thus outperform our SPS, but at a certain channel loss (>3.3 dB for the NV and >6.4 dB for the SiV, cf figure 4, translating into distances >8 km and >16 km using a typical transmission of light through air in sea level of 0.4 dB km^{-1} [38]) the SPS provides higher secure key rates and longer achievable transmission distances. This is due to a lower number of multiphoton events in a true SPS compared to an attenuated classical pulse of the same mean photon number. However, for the parameters achieved with single photon sources based on defect centres an attenuated laser together with the decoy state protocol is still favourable over our SPS regarding maximum key rates and achievable distances. This is because the obtained efficiencies of the SPS are not high enough and at the same time the $g^{(2)}(0)$ value not low enough to outperform WCP together with the decoy state protocol (cf section 6).

In this context, it is also interesting to note that even SPS sometimes have to be attenuated to reduce the small, but in a real source still existing fraction of multi-photon events to achieve the maximal possible transmission distance [33]. Even with high source efficiency, thus high mean photon number per excitation, security can be compromised at certain distances if the $g^{(2)}(0)$ value is not low enough. In fact for every $g^{(2)}(0)$ value and a given dark count rate of the detectors, the maximal mean photon number to realize the longest distances can be estimated after the following formula, taken from [33]:

$$\mu_c = \sqrt{\frac{2p_{dc}}{g^{(2)}(0)}}. \tag{3}$$

The ideal case would be to have a SPS which is above this critical mean photon number and to attenuate it in order to achieve the best rates at any distance. For our NV centre, we have an efficiency of 0.029 and a $g^{(2)}(0)$ of 0.09 (cf section 3.1). The critical mean photon number for this value of $g^{(2)}(0)$ is 0.039, a little above the given efficiency. There are examples of NV centres with higher efficiencies [20] which would surpass their critical mean photon number. For the SiV and its $g^{(2)}(0)$ value of 0.04, the efficiency of 0.012 (cf section 3.2) is below its critical mean photon number of 0.035 due to the low quantum efficiency of the SiV.

6. Discussion and conclusion

Our measurements have shown that there are severe constraints regarding the applicability of true single photon sources in QKD applications. Major requirements are a short lifetime, a quantum efficiency near unity, and a strong suppression of multi-photon events. Examples for sophisticated photon extraction architectures are plasmonically enhanced single photon sources [39], layered dielectric structures [40] or three-dimensional light guiding microstructures [41]. Since defect centres in NDs are point-like sources which can be easily integrated in such structures, collection efficiencies into a usable output mode exceeding 95% are realistic. In this case the internal quantum efficiency would still be a limitation. Recent studies [42, 43] have shown that the quantum efficiency may vary significantly within different NDs, but possibly emitters with more than 90% can be selected. An approach to enhance this requires enhancement of the radiative rate due to the Purcell effect [19, 44] which is technically more challenging for a room-temperature emitter [18]. For a higher suppression of multi-photon events and thus a lower g2(0), improving the signal-to-noise ratio by improving the collection and excitation efficiency through an appropriate optical setup of the SPS would be an important

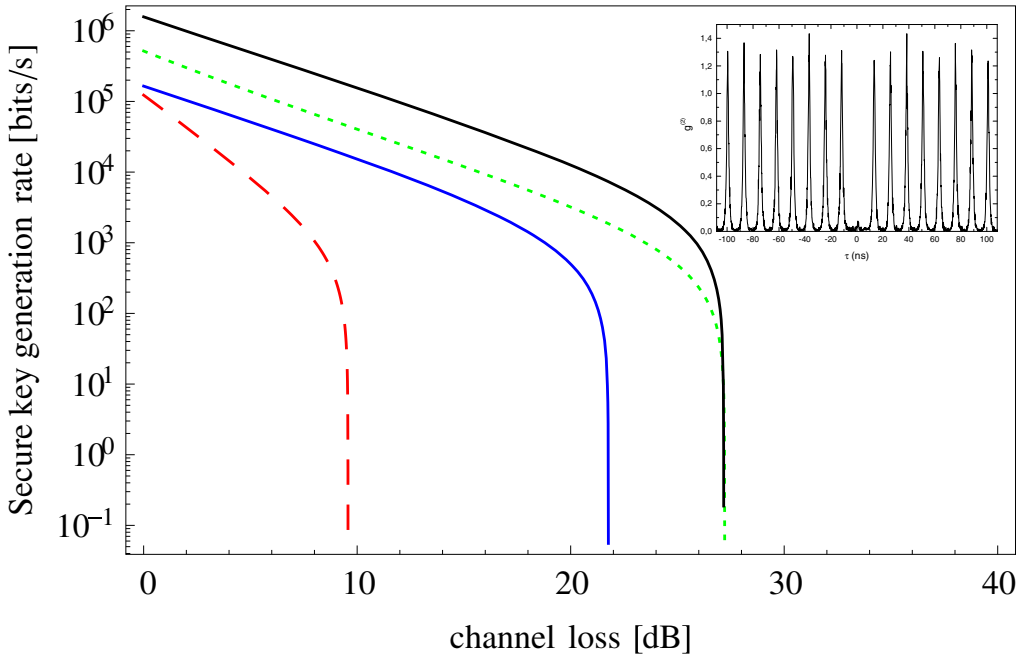

Figure 5. Secure key rates as a function of the channel losses of QKD experiments with defect centres with ideal, realistic features. For these sources, quantum efficiencies of 95% and photon yields of 10% (blue curve) and 95% (black curve) are assumed. The $g^2(0)$ value is 0.005 (blue curve) and 0.0005 (black curve). For comparison, an attenuated laser without (dashed red curve) and with (dotted green curve) decoy state protocol is depicted as well. The repetition rate is 20 MHz for all sources. The inset shows the $g^{(2)}$ value for a SiV for pulsed excitation at a repetition rate of 80 MHz. The count rate is 230 kcps with $g^{(2)}(0) < 0.1$.

step [20]. Also, near resonant excitation could be beneficial. Finally, it should be easier to suppress multiphoton events if the emission is narrow band (e.g. as in the SiV [10] or Cr centre [21] compared with the NV centre) and allows for better filtering of the signal against the background. A suppression of multi-photon events should be easier if the emission is narrow band (e.g. as in the SiV or Cr centre compared with the NV centre) and allows for better filtering of the signal against the background.

In figure 5, we estimated the maximum possible secure key generation rates for a possible future single photon source based on defect centres with enhanced efficiencies and lower probability of emitting multiple photons at a time. For this, we used a realistic repetition rate of 20 MHz.

As already mentioned, the SiV would allow for much higher excitation rates than shown here, which would lead to much higher key rates. The inset of figure 5 shows the $g^{(2)}$ value for an SiV for pulsed excitation at a repetition rate of 80 MHz, featuring a $g^{(2)}(0) < 0.1$ at a count rate of 230 kcps.

Figure 5 demonstrates that single photon sources based on defect centres in diamond could outperform attenuated light sources in the future under optimistic but not unrealistic assumptions.

In general, our QKD testbed allows for evaluations and feasibility tests of quantum light sources as stepping stones for a technology to move from research testbeds to mainstream

operations. A testbed is a step in between proof-of-principle experiments and novel commercial components outperforming existing ones. Often some specific problems with a system under study are only apparent and can only by attacked in a realistic architecture. Examples are possible side-channel attacks as a potential problem with any single photon source with a wide spectrum. Such and similar problems should be studied in testbeds before quantum light sources can be accepted as commercial products. Feasibility and cost-efficiency depend on the application and have to be well balanced. For example a recent demonstration of entanglement between distant NV centres [45] has introduced this system as platform for quantum repeaters [46]. If no practical alternative to long-distance QKD appears then cost might not be the main concern. Instead increasing the efficiency, stability, and maintenance-free operation are the main parameters to be optimized. The latter two have been addressed in [47] and are also crucial for possible air- or space-based single photon sources. Finally, novel cheaper ways to fabricate efficient single photon sources based on defect centres in plastic structures have been explored [41]. In conclusion there could be several new architectures of QIP where efficient quantum light sources are needed [48] in addition to protocols which allow for classical attenuated sources.

In summary, we implemented a QKD experiment with a compact SPS setup using defect centres. The setup of the source is such that it can easily be deployed in various QIP experiments. NV and SiV centres are used and can easily be interchanged within the experiment. SiV centres are potentially interesting for QIP applications due to their narrow spectral emission bandwidth but still suffer from drawbacks concerning their efficiency and their stability, which have to be overcome in the future. Together with a thorough security analysis of the QKD experiment, taking into account the source efficiency as well as its $g^{(2)}(0)$ value, we discussed the requirement to test quantum light sources in realistic architectures.

Acknowledgments

Funding by BMBF (QuaHL-ReP) and DFG (SFB787) is acknowledged by HU Berlin. CB and his co-workers from Universität des Saarlandes thank the Bundesministerium für Bildung und Forschung within the projects EphQuaM (contract 01BL0903) and QuOReP (contract 01BQ1011) for their financial support. We thank M Fischer, S Gsell and M Schreck (University of Augsburg) for supplying the CVD ND samples containing SiV centres. T Schröder also acknowledges support by the Alexander von Humboldt Stiftung.

References

[1] Gisin N, Ribordy G, Tittel W and Zbinden H 2002 Quantum cryptography *Rev. Mod. Phys.* **74** 145–95

[2] Sangouard N, Simon C, Minar J, Zbinden H, de Riedmatten H and Gisin N 2007 Long-distance entanglement distribution with single-photon sources *Phys. Rev.* A **76** 050301

[3] Dixon A R, Yuan Z L, Dynes J F, Sharpe A W and Shields A J 2010 Continuous operation of high bit rate quantum key distribution *Appl. Phys. Lett.* **96** 161102

[4] Tobias S-M *et al* 2007 Experimental demonstration of free-space decoy-state quantum key distribution over 144 km *Phys. Rev. Lett.* **98** 010504

[5] Hwang W-Y 2003 Quantum key distribution with high loss: toward global secure communication *Phys. Rev. Lett.* **91** 057901

[6] Lo H-K, Ma X and Chen K 2005 Decoy state quantum key distribution *Phys. Rev. Lett.* **94** 230504

[7] Intallura P M, Ward M B, Karimov O Z, Yuan Z L, See P, Shields A J, Atkinson P and Ritchie D A 2007 Quantum key distribution using a triggered quantum dot source emitting near 1.3 μm *Appl. Phys. Lett.* **91** 161103

[8] Heindel T *et al* 2012 Quantum key distribution using quantum dot single-photon emitting diodes in the red and near infrared spectral range *New J. Phys.* **14** 083001

[9] Kurtsiefer C, Mayer S, Zarda P and Weinfurter H 2000 Stable solid-state source of single photons *Phys. Rev. Lett.* **85** 290–3

[10] Neu E, Steinmetz D, Riedrich-Möller J, Gsell S, Fischer M, Schreck M and Becher C 2011 Single photon emission from silicon-vacancy colour centres in chemical vapour deposition nano-diamonds on iridium *New J. Phys.* **13** 025012

[11] Claudon J, Bleuse J, Malik N S, Bazin M, Jaffrennou P, Gregersen N, Sauvan C, Lalanne P and Gérard J-M 2010 A highly efficient single-photon source based on a quantum dot in a photonic nanowire *Nature Photon.* **4** 174–7

[12] Siyushev P, Pinto H, Vörös M, Gali A, Jelezko F and Wrachtrup J 2013 Optically controlled switching of the charge state of a single nitrogen-vacancy center in diamond at cryogenic temperatures *Phys. Rev. Lett.* **110** 167402

[13] Hossain F M, Doherty M W, Wilson H F and Hollenberg L C L 2008 *Ab initio* electronic and optical properties of the N–V^- center in diamond *Phys. Rev. Lett.* **101** 226403

[14] Manson N B, Harrison J P and Sellars M J 2006 Nitrogen-vacancy center in diamond: model of the electronic structure and associated dynamics *Phys. Rev.* B **74** 104303

[15] Beveratos A, Kühn S, Brouri R, Gacoin T, Poizat J-P and Grangier P 2002 Room temperature stable single-photon source *Eur. Phys. J.* D **18** 191–6

[16] Mizuochi N *et al* 2012 Electrically driven single-photon source at room temperature in diamond *Nature Photon.* **6** 299–303

[17] Neu E, Agio M and Becher C 2012 Photophysics of single silicon vacancy centers in diamond: implications for single photon emission *Opt. Express* **20** 19956–71

[18] Albrecht R, Bommer A, Deutsch C, Reichel J and Becher C 2013 Coupling of a single nitrogen-vacancy center in diamond to a fiber-based microcavity *Phys. Rev. Lett.* **110** 243602

[19] Wolters J, Schell A W, Kewes G, Nüsse N, Schoengen M, Döscher H, Hannappel T, Löchel B, Barth M and Benson O 2010 Enhancement of the zero phonon line emission from a single nitrogen vacancy center in a nanodiamond via coupling to a photonic crystal cavity *Appl. Phys. Lett.* **97** 141108

[20] Schröder T, Gädeke F, Banholzer M J and Benson O 2011 Ultrabright and efficient single-photon generation based on nitrogen-vacancy centres in nanodiamonds on a solid immersion lens *New J. Phys.* **13** 055017

[21] Aharonovich I, Castelletto S, Johnson B C, McCallum J C, Simpson D A, Greentree A D and Prawer S 2010 Chromium single-photon emitters in diamond fabricated by ion implantation *Phys. Rev.* B **81** 121201

[22] Aharonovich I, Castelletto S, Simpson D A, Greentree A D and Prawer S 2010 Photophysics of chromium-related diamond single-photon emitters *Phys. Rev.* A **81** 043813

[23] Beveratos A, Brouri R, Gacoin T, Villing A, Poizat J-P and Grangier P 2002 Single photon quantum cryptography *Phys. Rev. Lett.* **89** 187901

[24] Alléaume R, Treussart F, Messin G, Dumeige Y, Roch J-F, Beveratos A, Brouri-Tualle R, Poizat J-P and Grangier P 2004 Experimental open-air quantum key distribution with a single-photon source *New J. Phys.* **6** 92

[25] Rabeau J R, Stacey A, Rabeau A, Prawer S, Jelezko F, Mirza I and Wrachtrup J 2007 Single nitrogen vacancy centers in chemical vapor deposited diamond nanocrystals *Nano Lett.* **7** 3433–7

[26] Hanbury Brown R and Twiss R Q 1956 A test of a new type of stellar interferometer on Sirius *Nature* **178** 1046–8

[27] Schönau T, Riecke S M, Lauritsen K and Erdmann R 2011 Amplification of ps-pulses from freely triggerable gain-switched laser diodes at 1062 nm and second harmonic generation in periodically poled lithium niobate *Proc. SPIE* **7917** 791707

[28] Buttler W T, Hughes R J, Lamoreaux S K, Morgan G L, Nordholt J E and Peterson C G 2000 Daylight quantum key distribution over 1.6 km *Phys. Rev. Lett.* **84** 5652–5
[29] Arend C 2011 Kontinuierliche und zeitabhängige Spektroskopie an Farbzentren in Diamant. Diplomarbeit, Naturwissenschaftlich-Technische Fakultät II, Physik und Mechatronik, Universität des Saarlandes
[30] Bennett C H and Brassard G 1984 Quantum cryptography: public key distribution and coin tossing *Proc. IEEE Int. Conf. on Computers, Systems and Signal Processing, Bangalore* p 175
[31] Wahl M, Leifgen M, Berlin M, Röhlicke T, Rahn H-J and Benson O 2011 An ultrafast quantum random number generator with provably bounded output bias based on photon arrival time measurements *Appl. Phys. Lett.* **98** 171105
[32] Brassard G and Salvail L 1994 Secret-key reconciliation by public discussion *Advances in Cryptology—EUROCRYPT'93* (*Lecture Notes in Computer Science* vol 765) ed T Helleseth (Berlin: Springer) pp 410–23
[33] Waks E, Santori C and Yamamoto Y 2002 Security aspects of quantum key distribution with sub-Poisson light *Phys. Rev.* A **66** 042315
[34] Gottesman D, Lo H-K, Lütkenhaus N and Preskill J 2004 Security of quantum key distribution with imperfect devices *Quantum Inform. Comput.* **4** 325–60
[35] Shannon C E 1948 A mathematical theory of communication *Bell Syst. Tech. J.* **27** 379–423, 623–56
[36] Lütkenhaus N 2000 Security against individual attacks for realistic quantum key distribution *Phys. Rev.* A **61** 052304
[37] Ma X, Qi B, Zhao Y and Lo H-K 2005 Practical decoy state for quantum key distribution *Phys. Rev.* A **72** 012326
[38] Giggenbach D 2005 Optimierung der optischen Freiraumkommunikation durch die turbulente Atmosphäre—Focal Array Receiver *Dissertation* DLR Oberpfaffenhofen, Institut für Kommunikation und Navigation, Digitale Netze
[39] Schietinger S, Barth M, Aichele T and Benson O 2009 Plasmon-enhanced single photon emission from a nanoassembled metal-diamond hybrid structure at room temperature *Nano Lett.* **9** 1694–8
[40] Lee K G, Chen X W, Eghlidi H, Kukura P, Lettow R, Renn A, Sandoghdar V and Götzinger S 2011 A planar dielectric antenna for directional single-photon emission and near-unity collection efficiency *Nature Photon.* **5** 166–9
[41] Schell A W, Kaschke J, Fischer J, Henze R, Wolters J, Wegener M and Benson O 2013 Three-dimensional quantum photonic elements based on single nitrogen vacancy-centres in laser-written microstructures *Sci. Rep.* **3** 1577
[42] Frimmer M, Mohtashami A and Femius Koenderink A 2013 Nanomechanical method to gauge emission quantum yield applied to nitrogen-vacancy centers in nanodiamond *Appl. Phys. Lett.* **102** 121105
[43] Schell A W, Engel P and Benson O 2013 Probing the local density of states in three dimensions with a scanning single quantum emitter arXiv:1303.0814v1 [quant-ph]
[44] Riedrich-Möller J *et al* 2012 One- and two-dimensional photonic crystal microcavities in single crystal diamond *Nature Nanotechnol.* **7** 69–74
[45] Bernien H *et al* 2013 Heralded entanglement between solid-state qubits separated by three metres *Nature* **497** 86–90
[46] Briegel H-J, Dür W, Cirac J I and Zoller P 1998 Quantum repeaters: the role of imperfect local operations in quantum communication *Phys. Rev. Lett.* **81** 5932–5
[47] Schröder T, Engel P, Schmidt E and Benson O 2012 Integrated and compact fiber-coupled single-photon system based on nitrogen-vacancy centers and gradient-index lenses *Opt. Lett.* **37** 2901–3
[48] Sangouard N and Zbinden H 2012 What are single photons good for? *J. Mod. Opt.* **59** 1458–64